

Robust Discrete-Time Lateral Control of Racecars by Unknown Input Observers

Salvatore Pedone¹ and Adriano Fagiolini¹, *Member, IEEE*

Abstract—This brief addresses the robust lateral control problem for self-driving racecars. It proposes a discrete-time estimation and control solution consisting of a delayed unknown input-state observer (UIO) and a robust tracking controller. Based on a nominal vehicle model, describing its motion with respect to a generic desired trajectory and requiring no information about the surrounding environment, the observer reconstructs the total force disturbance signal, resulting from imperfect knowledge of the time-varying tire-road interface characteristics, presence of other vehicles nearby, wind gusts, and other model uncertainty. Then, the controller actively compensates the estimated force and asymptotically steers the tracking error to zero. The brief also presents a closed-loop stability proof of the method, ensuring perfect asymptotic estimation and tracking by the controlled vehicle. The proposed solution advantageously needs no a-priori information about the total disturbance boundedness, additional variables to model uncertainty, or observer parameters to be tuned. Its effectiveness and superiority to existing methods are studied in theory and shown in simulations where a full racecar model, based on the vehicle dynamics blockset, is required to track aggressive maneuvers. Through a faster and more accurate disturbance estimation, the solution robustly ensures better dynamic responses even with measurement noise.

Index Terms—Autonomous vehicles, extended state observer (ESO), input-state estimation, racecars, robust vehicle control, self-driving.

I. INTRODUCTION

THE motion of a vehicle is governed by the traction force, generated at the wheels, and all resistance forces that apply to it [1]. The traction force results from the complex interaction between the tire contact patch and the road. It nonlinearly depends on the driving motor torque and a set of parameters that vary with time and can only be identified for typical road typologies (cf., Burckhardt's [2] and Pacejka's [3] models). Resistance forces include the aerodynamic load losses and rolling resistance which have known expressions under nominal conditions. Yet, they still depend on coefficients whose accurate knowledge requires perfect modeling of the vehicle profile. Other external forces are disturbance signals, not easy to predict, such as wind gusts (normally modeled via stochastic Dryden winds [4]),

Manuscript received 15 December 2021; revised 20 July 2022; accepted 16 September 2022. This work was supported in part by the Ministero dell'Istruzione, dell'Università e della Ricerca (MIUR) "Dottorati innovativi a caratterizzazione industriale" under Project POC R&I 2014–2020. Recommended by Associate Editor S. Evangelou. (*Corresponding author: Adriano Fagiolini.*)

The authors are with the Mobile and Intelligent Robots@Panormous Laboratory (MIRPALab), Department of Engineering, University of Palermo, 90128 Palermo, Italy (e-mail: salvatore.pedone@unipa.it; fagiolini@unipa.it).

Color versions of one or more figures in this article are available at <https://doi.org/10.1109/TCST.2022.3214054>.

Digital Object Identifier 10.1109/TCST.2022.3214054

airflow-turbulence due to surrounding vehicles, and road bank angle changes.

To obtain precise motion regulation for a vehicle, robust control techniques are naturally advocated. The technique presented in [5] achieved improved performance on a four-wheel vehicle. A comparison of the immersion and invariance principle, sliding mode control, and passivity techniques is reported [6]. These methods require a-priori knowledge of the maximum disturbance magnitude, involve high control gains and integral terms, or discontinuous control signals, which may result in over-conservative strategies, needing bigger efforts to prevent instability. Another way to cope with uncertainty is to estimate and compensate for the actual disturbance. A cascaded backstepping control method with an augmented observer is proposed in [7] to control the lateral dynamics of an autonomous vehicle in the presence of disturbance. However, it assumes that the disturbance slowly changes, thus limiting its applicability and effectiveness in general. Traditional disturbance estimation approaches, based on extended Kalman filters (EKFs), suffer from known disadvantages due to the necessity to calibrate noise covariance matrices and introduce additional states, whose dynamics can only be based on the generic random walk [8]. Beyond the fact that a convergence proof in the general scenario cannot be found, they result in over-delayed estimation or, even worse, divergent estimation behaviors (see the discussion in [9]).

Other more effective solutions rely on disturbance observer-based (DOB) approaches [10], [11], [12], [13]. Built upon a nominal vehicle model, they reach great estimation performance when the system state is entirely measurable. In fact, when the state is not fully accessible, they require an additional state observer, introducing further complexity and reducing the solution's efficiency. To overcome this limitation and simultaneously estimate disturbance inputs and states, extended state observers (ESOs) come in handy, which, similar to EKFs, model the deviation with respect to a nominal behavior as additional states and only require tuning a set of control parameters [14], [15], [16]. Despite their simplicity, they involve again high-gain parameters that make them often too sensitive to measurement noise and lead to peaky estimations. Also, they assume a small or negligible change over time of the disturbance signals [17]. Closely related to the ESOs is the active disturbance rejection control (ADRC) technique [18], [19], [20], [21]. It is a robust control method assuming that parameter and model uncertainties are modeled as a disturbance input vector, estimated via an ESO, and finally compensated via a state-feedback control law [14]. Despite its simplicity, its closed-loop stability remains strongly linked to the underlying ESO's primary assumption that the disturbance

acting on the system has a negligible rate of change, which leads to worse estimation performance in systems with fast varying disturbances.

Within this context, this brief proposes a novel discrete-time robust control solution for racecar lateral dynamics, which uses a linear unknown input-state observer (UIO) [22]. Built upon a double-track nominal model, the observer reconstructs the total force disturbance signal, resulting from imperfect knowledge of the time-varying tire-road interface characteristics, the presence of other nearby vehicles, wind gusts, model reduction, and uncertainty. Then, a controller actively compensates the estimated force and asymptotically steers the tracking error to zero. Among other advantages, the proposed solution needs no a-priori information about the total disturbance boundedness, additional variables to model uncertainty, or tuning of observer parameters. It allows faster and more accurate disturbance estimation and better dynamic response.

Contribution: The brief's contribution is at least fourfold. First, by starting from the so-called double-track system, the brief derives a nominal model of the lateral racecar dynamics, in a form where the input-disturbance and state estimation can be addressed by using delayed UIO theory; second, a robust control law is devised which uses state and disturbance estimates to ensure perfect asymptotic tracking of any desired trajectory, and the full state closed-loop asymptotic stability is formally proved with convergence speed guarantees; third, the superiority of the proposed method to existing state-of-the-art solutions is shown; finally, the effectiveness, the robustness, and the real-time implementability of the proposed solution are tested by using the models of MATLAB/Simulink's Vehicle Dynamics Blockset [23] and a Raspberry PI 4 system.

II. MODEL FORMALIZATION AND PROBLEM STATEMENT

Consider a rear-wheel drive, front-steering racecar with mass m and inertia J , moving along a flat horizontal road, i.e., with zero bank angle. The in-plane lateral dynamics of the vehicle can be described, in a noninertial frame attached to it, by the double-track model [1] that reads

$$\begin{aligned} m(\ddot{y} + u\dot{\psi}) &= Y_1(\delta_v) + Y_2(\delta_v) + F_w \\ J\ddot{\psi} &= a_1 Y_1(\delta_v) + a_2 Y_2(\delta_v) + \chi_w \end{aligned} \quad (1)$$

where y is its lateral position, ψ is its heading angle, a_1 and a_2 are its wheelbases, Y_1 and Y_2 are the front and rear lateral forces applied at its center of mass, δ_v is the front steering angle and system input, F_w and χ_w are the lateral wind force and moment, and u is its longitudinal speed, which can be considered a time-varying parameter, resulting from the control of its longitudinal dynamics. The lateral forces Y_1 and Y_2 can be decomposed as follows:

$$\begin{aligned} Y_1 &= F_{y_{11}}(\delta_v) \cos(\delta_{11}(\delta_v)) + F_{y_{12}}(\delta_v) \cos(\delta_{12}(\delta_v)) \\ Y_2 &= F_{y_{21}} + F_{y_{22}} \end{aligned}$$

where $F_{y_{ij}}$ are the front ($i = 1$) and rear ($i = 2$) forces applied at the left ($j = 1$) and right ($j = 2$) tires, respectively, and are nonlinear functions of the front wheel steer angles δ_{1j} . Moreover, refer to Fig. 1 and assume that a global positioning system (GPS) sensor is used to measure the (X, Y) coordinates

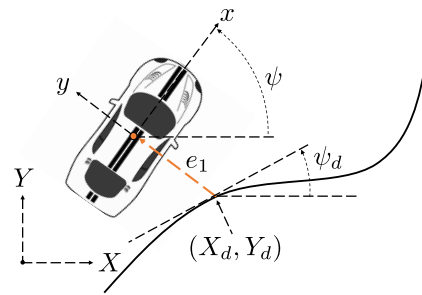


Fig. 1. Depiction of the vehicle schematic, desired path, and coordinate frames.

of the vehicle center of mass in an Inertial frame. Given the (X_d, Y_d) coordinates of a point on a desired trajectory to be tracked, with a curvature radius R , if the vehicle is required to track such trajectory and, simultaneously, vanish its lateral position y , while moving at a longitudinal speed u , a lateral position error e_1 can be introduced as the projection of the error vector $(X, Y)^T - (X_d, Y_d)^T$ along the lateral direction unit vector $(-\sin \psi, \cos \psi)^T$, i.e., $e_1 = (Y - Y_d) \cos \psi - (X - X_d) \sin \psi$. Indicating with $a_{y_d} = u^2/R = u\dot{\psi}_d$ an approximated desired lateral acceleration in body frame, the corresponding lateral acceleration error reads [1] as follows:

$$\begin{aligned} \ddot{e}_1 &= a_y - a_{y_d} = \ddot{y} + u\dot{\psi} - a_{y_d} \\ &= \frac{1}{m}(Y_1(\delta_v) + Y_2(\delta_v) + F_w) - a_{y_d} \end{aligned} \quad (2)$$

where the actual lateral acceleration a_y has been expanded as $a_y = \ddot{y} + \dot{\psi}u$ and the first equation in (1) has been used.

Furthermore, achieving precise and complete characterization of the nonlinear and possibly time-varying functions Y_1 and Y_2 requires ad hoc identification procedures which also need to be repeated over time [1]. Beyond that, the wind force and moment signals are only predictable via statistical models and hence their actual values over time remain unknown. Therefore, it is convenient to obtain a nominal vehicle model based on quantities that can be easily identified. For this purpose, one recalls that the lateral forces at the tires depend on the respective wheel slip angles α_{ij} , for $i, j = 1, 2$; such dependence can be approximated, for small α_{ij} , as $F_{y_{ij}} = C_{ij} \alpha_{ij}$, where C_{ij} are the tires' cornering stiffness coefficients, which are known with good accuracy. Moreover, the wheel slip angles can be expressed by the following formulas:

$$\begin{aligned} \alpha_{1j} &= \delta_{1j}(\delta_v) - \arctan((v + r a_1)/(u + (-1)^j r t_1/2)) \\ \alpha_{2j} &= -\arctan((v - r a_2)/(u + (-1)^j r t_2/2)) \end{aligned}$$

with t_1 and t_2 being the front and rear vehicle tracks, $v = \dot{y}$ and $r = \dot{\psi}$ are the lateral and yaw speeds. While the functions $\delta_{1j}(\delta_v)$ are highly nonlinear, for small values of their argument, the following second-order Taylor expansions can be used [1]:

$$\delta_{1j}(\delta_v) = (-1)^j \delta_1^0 + \tau \delta_v + (-1)^{j-1} \frac{\beta t_1}{2l} \tau^2 \delta_v^2 + \nu$$

with δ_1^0 , l , τ , and β being the static toe angle, the total wheelbase, the steering gear ratio, and the Ackermann coefficient, respectively, and ν the approximation error signal. In light

where $\hat{Z}_{k-L} = (\hat{e}_{k-L}, \hat{e}_{k-L})^T$, $\mathbb{Y}_k^L = (e_k, e_{k-1}, e_{k-2})^T$, and

$$E = \begin{pmatrix} \sigma_1 & 0 \\ 0 & \sigma_2 \end{pmatrix}, \quad F = \begin{pmatrix} -\sigma_1 & 1 & 0 \\ \frac{\sigma_2}{\lambda} & -\frac{1+\sigma_2}{\lambda} & \lambda \end{pmatrix}$$

$$G = \begin{pmatrix} 1 \\ 0 & \frac{1}{\lambda} & 0 \end{pmatrix} \quad (9)$$

with σ_1 and σ_2 being free constants such that $|\sigma_1|, |\sigma_2| < 1$, is a DUIO for the model in (4) with reconstruction delay $L = 2$. That is, the filter in (8) can asymptotically reconstruct the full system state $Z_{k-L} = (e_{k-L}, \dot{e}_{k-L})^T$ and the unknown disturbance w_{k-L} .

Proof: To design a DUIO of the form in (6) for the racecar model in (4) one need first to introduce a new input $U_{k-L} = b \delta_{k-L} + w_{k-L}$, with $b = \bar{C}_1 \bar{\tau} / \bar{m}$, collecting both the known control δ_k and the disturbance w_k , and its corresponding input matrix $B = \lambda(0, 1)^T$. Choosing the output and direct matrices are $C = C_k$ and $D = D_k$, the smallest integer satisfying Proposition 2 is $L = 2$, for which it holds $\text{rank}(\mathbb{H}^2) - \text{rank}(\mathbb{H}^1) = 1 = m$ since $\mathbb{H}^1 = 0_{2 \times 2}$ and

$$\mathbb{H}^2 = \begin{pmatrix} D & 0 & 0 \\ CB & D & 0 \\ CAB & CB & 0 \end{pmatrix} = \begin{pmatrix} 0 & 0 & 0 \\ 0 & 0 & 0 \\ \lambda^2 & 0 & 0 \end{pmatrix}.$$

Consequently, the output history can be chosen as $\mathbb{Y}_k^2 = (e_k, e_{k-1}, e_{k-2})^T$. Condition A1 in Section III-A implies that matrix F belong to the left-nullspace of the last columns of matrix \mathbb{H}^2 , which are given by $P = \begin{pmatrix} 0_{2 \times 2} \\ \mathbb{H}^1 \end{pmatrix}$. To determine F , consider first a matrix \bar{N} whose rows form a basis for the left-nullspace of \mathbb{H}^1 , so that $\begin{pmatrix} I_p & 0_{p \times 2} \\ 0_{2 \times p} & \bar{N} \end{pmatrix}$ is a matrix whose rows form a basis for the left-nullspace of P . Constant p equals the unity since the system output e_k is scalar. Given the null value of \mathbb{H}^1 , for this system, it suffices to choose $\bar{N} = I_{2 \times 2}$. Furthermore, for any invertible matrix W , we can define a matrix $N = W \begin{pmatrix} 1 & 0_{1 \times 2} \\ 0_{2 \times 1} & \bar{N} \end{pmatrix} = W I_{3 \times 3}$, whose rows also form a basis for the left nullspace of P . Therefore, given the one-step observability matrix (see Section III-A), $\mathbb{O}^1 = \begin{pmatrix} C \\ CA \end{pmatrix} = \begin{pmatrix} 1 & 0 \\ \lambda \end{pmatrix}$, to find W , one can first note that $N \begin{pmatrix} D & 0 \\ \mathbb{O}^1 B & \mathbb{H} \end{pmatrix} = W \begin{pmatrix} D & 0 \\ \bar{N} \mathbb{O}^1 B & 0_{2 \times 1} \end{pmatrix}$. Moreover, as Proposition 2 is satisfied for a delay $L = 2$, the first columns of \mathbb{H}^2 are linearly independent, which implies that the matrix $\begin{pmatrix} D & 0 \\ \bar{N} \mathbb{O}^1 B & 0_{2 \times 1} \end{pmatrix}$ have rank equal to the unity. Direct computation of the above matrix shows indeed that $\begin{pmatrix} D & 0 \\ \bar{N} \mathbb{O}^1 B & 0_{2 \times 1} \end{pmatrix} = \begin{pmatrix} 0 & 0 & \lambda^2 \\ 0 & 0 & 0 \end{pmatrix}^T$. Now, one can choose matrix W so that the last rows form a left-inverse of the last above matrix, while the upper ones form a basis of its left-nullspace. A possible choice for W is then $W = \text{diag}(1, 1, 1/\lambda^2)$, which leads also to a matrix N satisfying the expression

$$N \mathbb{H}^2 = \begin{pmatrix} 0 & 0 & 0 \\ 0 & 0 & 0 \\ 1 & 0 & 0 \end{pmatrix}.$$

This fact finally leads to derive that it holds $N = W$. Furthermore, based again on Condition A1, matrix F can be

factorized as $F = \bar{F} N$, with $\bar{F} = (\bar{F}_1, \bar{F}_2)$ and \bar{F}_2 being a vector. Explicitly writing Condition A1 yields

$$(\bar{F}_1 \bar{F}_2) \begin{pmatrix} 0 & 0 & 1 \\ 0 & 0 & 0 \end{pmatrix}^T = (B \quad 0_{2 \times 1} \quad 0_{2 \times 1}) = \begin{pmatrix} 0 & 0 & 0 \\ \lambda & 0 & 0 \end{pmatrix}$$

which allows obtaining the solution $\bar{F}_2 = B = (0, \lambda)^T$ and \bar{F}_1 a still free design matrix.

Moving now on to the satisfaction of Condition A2, we can directly obtain $E = A - F \mathbb{O}^2 = A - (\bar{F}_1, B) N \mathbb{O}^2$. Splitting the rows of the matrix $N \mathbb{O}^2$ on the right-hand side into two sub-matrices S_1 and S_2 , that is,

$$N \mathbb{O}^2 = \begin{pmatrix} 1 & 0 & 0 \\ 0 & 1 & 0 \\ 0 & 0 & 1/\lambda^2 \end{pmatrix} \begin{pmatrix} 1 & 0 \\ 1 & \lambda \\ 1 & 2\lambda \end{pmatrix} = \begin{pmatrix} 1 & 0 \\ 1 & \lambda \\ 1/\lambda^2 & 2/\lambda \end{pmatrix} = \begin{pmatrix} S_1 \\ S_2 \end{pmatrix}$$

with $S_1 = \begin{pmatrix} 1 & 0 \\ 1 & \lambda \end{pmatrix}$, $S_2 = (1/\lambda^2 \quad 2/\lambda)$, allows further expanding the expression of matrix E as follows:

$$E = A - B S_2 - \bar{F}_1 S_1 = \begin{pmatrix} 1 & \lambda \\ -1/\lambda & -1 \end{pmatrix} - \bar{F}_1 \begin{pmatrix} 1 & 0 \\ 1 & \lambda \end{pmatrix}.$$

To finally satisfy also Condition A3, one can impose matrix E to be given by a Schur diagonal matrix as in (9). This condition can be attained by choosing the remaining part of matrix F as $\bar{F}_1 = \begin{pmatrix} -\sigma_1 & 1 \\ \sigma_2/\lambda & -(1+\sigma_2)/\lambda \end{pmatrix}$. By the above choices, the solution of the dynamics for the estimation error $\tilde{e}_k = \hat{Z}_{k-L} - Z_{k-L}$ is

$$\tilde{e}_{k+1} = E \tilde{e}_k \quad (10)$$

which has a convergent behavior with a speed of convergence directly dependent on the free parameters σ_1 and σ_2 .

Having guaranteed the convergence of the state estimation error, the unknown input disturbance w_k can be retrieved as follows. First, (4) can be rearranged as follows:

$$\begin{pmatrix} Z_{k-L+1} - A_k Z_{k-L} - B_k \delta_{k-L} \\ y_{k-L} - C Z_{k-L} \end{pmatrix} = \begin{pmatrix} W_k \\ D_k \end{pmatrix} w_{k-L} \quad (11)$$

and its both sides can be left-multiplied by the pseudo-inverse of $(W_k^T, D_k^T)^T$, i.e., matrix G in (9). Doing so and then replacing the state with its estimate yields

$$\hat{w}_{k-L} = G \begin{pmatrix} \hat{Z}_{k-L+1} - A_k \hat{Z}_{k-L} - B_k \delta_{k-L} \\ y_{k-L} - C \hat{Z}_{k-L} \end{pmatrix}. \quad (12)$$

Finally, writing explicitly the term $y_{k-L} - C \hat{Z}_{k-L}$ allows reaching the formula in (8) and concludes the proof. ■

C. Design of the Robust Lateral Position Control

As a second step, leveraging on the data reconstructed by the above designed DUIO, a robust lateral position controller for the steering angle input δ_k is derived, which ensures e_k 's convergence independently of all model uncertainty and external disturbance. This is formalized in the following second main result.

Theorem 2: Given the dynamics of the racecar model in (4), the feedback steering angle control law

$$\delta_k = -\frac{\bar{m}}{\bar{C}_1 \bar{\tau}} (K \hat{Z}_{k-L} + \hat{w}_{k-L}) \quad (13)$$

where \hat{Z}_{k-L} and \hat{w}_{k-L} are the state and disturbance estimates from the DUIO in (8) and where $K = (k_1, k_2)$ is a free control gain matrix, ensures robust, and global asymptotic convergence of the state estimation error \tilde{e}_k and robust and global uniform bounded stability of the racecar state Z_k around the origin, with a bound decreasing at least linearly with the sampling time λ .

Proof: The full dynamics of the racecar in (4) and the DUIO in (8) is

$$\begin{pmatrix} Z_{k+1} \\ \tilde{e}_{k+1} \end{pmatrix} = \begin{pmatrix} A_k & 0_{2 \times 2} \\ 0_{2 \times 2} & E \end{pmatrix} \begin{pmatrix} Z_k \\ \tilde{e}_k \end{pmatrix} + \begin{pmatrix} B_k \delta_k + W_k w_k \\ 0_{2 \times 1} \end{pmatrix} \quad (14)$$

in which the state estimation error dynamics is independent of the controlled input δ_k and the disturbance signal w_k (cf., the last set of equations). This fact implies that the convergence of \tilde{e}_k in the closed-loop system is again ensured by E being Schur, and that, after convergence, $\hat{Z}_{k-L} \simeq Z_{k-L}$ and $\hat{w}_{k-L} \simeq w_{k-L}$. Consequently, the feedback law in (13) becomes $\delta_k \simeq -\bar{m}/(\bar{C}_1 \bar{\tau})(K Z_{k-L} + w_{k-L})$. Hence, closing the loop on (14) with such a feedback law yields

$$\begin{pmatrix} Z_{k+1} \\ \tilde{e}_{k+1} \end{pmatrix} = \begin{pmatrix} A_k & 0_{2 \times 2} \\ 0_{2 \times 2} & E \end{pmatrix} \begin{pmatrix} Z_k \\ \tilde{e}_k \end{pmatrix} - \begin{pmatrix} B_v \\ 0_{2 \times 1} \end{pmatrix} (K Z_{k-L} - \tilde{w}_k) \quad (15)$$

where $B_v = \lambda(0, 1)^T = W_k$ and $\tilde{w}_k = w_k - w_{k-L}$ is the disturbance estimation error. Using the factorization $A_k Z_k - B_v K Z_{k-L} + B_v \tilde{w}_k = (A_k - B_v K) Z_k + \phi_k$, with $\phi_k = B_v(K(Z_k - Z_{k-L}) + \tilde{w}_k)$ allows rewriting (15) as follows:

$$\begin{pmatrix} Z_{k+1} \\ \tilde{e}_{k+1} \end{pmatrix} = A_c \begin{pmatrix} Z_k \\ \tilde{e}_k \end{pmatrix} + \begin{pmatrix} \mathbb{I}_{2 \times 2} \\ 0_{2 \times 1} \end{pmatrix} \phi_k \quad (16)$$

with

$$A_c = \begin{pmatrix} A_k - B_v K & -B_v K \\ 0_{2 \times 2} & E \end{pmatrix} = \begin{pmatrix} 1 & \lambda & 0 & 0 \\ -\lambda k_1 & \gamma_1 & -\lambda k_1 & -\lambda k_2 \\ 0 & 0 & \sigma_1 & 0 \\ 0 & 0 & 0 & \sigma_2 \end{pmatrix}$$

and $\gamma_1 = 1 - \lambda k_2$. It should be first noticed that the free solution of (16) can be made convergent, by properly allocating the eigenvalues of A_c . In this respect, matrix A_c is upper-block triangular and hence the set of its eigenvalues comprises those of the DUIO, σ_1 and σ_2 , and those of $A_k - B_v K$. The controllability matrix of the pair (A_k, B_v) is $\mathcal{R} = (B_v | A_k B_v) = \begin{pmatrix} 0 & \lambda^2 \\ \lambda & \lambda \end{pmatrix}$ and has full rank, which ensures the existence of a matrix K so that $A_k - B_v K$ has all eigenvalues within the unit circle and then generates asymptotically stable modes only. Furthermore, recall from [24] that for a small enough sampling time λ , it holds, for consecutive samples, $\hat{Z}_k \simeq \hat{Z}_{k-1}$ and $w_k \simeq w_{k-1}$ or equivalently

$$\|Z_k - Z_{k-1}\|_2 < p_Z(\lambda), \quad \|w_k - w_{k-1}\|_2 < p_w(\lambda) \quad (17)$$

with $p_Z, p_w \in \mathbb{R}^+$ diminishing with the decrease of λ and where $\|\cdot\|_2$ is the Euclidean norm. From the property in (17), derived from [24], it also follows $\delta_k \simeq \delta_{k-1} \simeq \delta_{k-L}$, which solves the algebraic dependence of w_k from δ_k . Analogously, it holds $y_k \simeq y_{k-1} \simeq y_{k-L}$. Moreover, recalling that $L = 2$, the term ϕ_k can be rewritten as $\phi_k = K(Z_k - Z_{k-1}) + K(Z_{k-1} -$

$Z_{k-2}) + w_k - w_{k-1} + w_{k-1} - w_{k-2}$, and thus can be upper bounded as follows:

$$\begin{aligned} \|\phi_k\|_2 &\leq \|B_v\|_2 \|K\|_2 \|Z_k - Z_{k-1}\|_2 \\ &\quad + \|B_v\|_2 \|K\|_2 \|Z_{k-1} - Z_{k-2}\|_2 \\ &\quad + \|w_k - w_{k-1}\|_2 + \|w_{k-1} - w_{k-2}\|_2 \\ &= \lambda(2 \|K\|_2 p_Z(\lambda) + 2 p_w(\lambda)). \end{aligned}$$

From the first set of equations in (16), we have

$$\begin{aligned} \|Z_{k+1}\| &\leq \|A_c Z_k\| + \|\phi_k\| \\ &\leq \|A_c Z_k\| + \lambda(2 \|K\|_2 p_Z(\lambda) + 2 p_w(\lambda)). \end{aligned}$$

Since A_c is Schur, the first addend in the equation above is contracting, i.e., $\|A_c Z_k\| < \|Z_k\|$ and hence, after a transient, the norm of the racecar state is only excited by the forcing term ϕ_k which decreases at least linearly with the decrease of λ .

Furthermore, as for the convergence of disturbance estimation error, \tilde{w}_k , from its definition, one can write as follows:

$$\begin{aligned} \tilde{w}_k &= G \begin{pmatrix} Z_{k+1} - A_k Z_k - B_k \delta_k \\ y_k - C Z_k \end{pmatrix} + \\ &\quad - G \begin{pmatrix} \hat{Z}_{k-L+1} - A_k \hat{Z}_{k-L} - B_k \delta_{k-L} \\ y_{k-L} - C \hat{Z}_{k-L} \end{pmatrix} \end{aligned}$$

which, after having defined the signals $v_k = \hat{Z}_{k-L} - Z_k$, $\eta_k = \delta_{k-L} - \delta_k$, and $\zeta_k = y_{k-L} - y_k$, becomes finally

$$\tilde{w}_k = G \begin{pmatrix} A_k v_k + B_k \eta_k - v_{k+1} \\ C v_k - \zeta_k \end{pmatrix}. \quad (18)$$

Again under the hypothesis of [24] for small delays, the signals v_k , η_k , and ζ_k are bounded, i.e. there exist constant upper-bounds, $S, V, T \in \mathbb{R}^+$, such that $\|v_k\|_2 \leq S$, $\|\eta_k\|_2 \leq V$, and $\|\zeta_k\|_2 \leq T$, for all k , and also convergent due to (17), i.e., for increasing values of k the upper bounds can be chosen as $S, V, T \rightarrow 0$. As a consequence, from (18), one can obtain

$$\begin{aligned} \|\tilde{w}_k\|_2^2 &\leq \|G\|_2^2 \left\| \begin{pmatrix} A_k v_k + B_k \eta_k - v_{k+1} \\ C v_k - \zeta_k \end{pmatrix} \right\|_2^2 \\ &\leq G_2^2 (\|A_k v_k + B_k \eta_k - v_{k+1}\|_2 + \|C v_k - \zeta_k\|_2)^2 \\ &\leq G_2^2 (\|A_k\|_2 S + \|B_k\|_2 V + S + \|C\|_2 S + T)^2 \\ &\leq G_2^2 ((\rho_A + 2)S + (\lambda \bar{C}_1 \bar{\tau} / \bar{m})V + T)^2 \end{aligned}$$

with $G_2 = 1/\lambda$ and $\rho_A = (\rho(A_k^T A_k))^{1/2}$, where $\rho(\cdot)$ indicates the spectral radius of a matrix. Therefore, the fact that $S, V, T \rightarrow 0$ also implies $\|\tilde{w}_k\|_2 \rightarrow 0$ and, in turn, $\tilde{w}_k \rightarrow 0$. Hence, the disturbance estimation error \tilde{w}_k asymptotically converges to zero with the same speed of the state estimation error \tilde{e}_k , which is specified by the free constants σ_1 and σ_2 of the DUIO. This concludes the proof. ■

Therefore, the DUIO-based control observes the system state and inputs at the time-step $k - L$, reconstructs the unknown disturbance \hat{w}_{k-L} , and finally determines the control action for the time step k steering the closed-loop system in (14) and allowing the sought asymptotic convergence to zero.

TABLE I

NOMINAL INERTIAL AND GEOMETRIC PARAMETERS OF A ROBOCAR FROM THE ROBORACE CHALLENGE [25]

Total Front cornering stiffness	C_1	$2.26 \cdot 10^5$ N/rad
Total Rear cornering stiffness	C_2	$2.82 \cdot 10^5$ N/rad
Front wheelbase	a_1	1.510 m
Rear wheelbase	a_2	1.288 m
Front track	t_1	1.714 m
Rear track	t_2	1.692 m
Vehicle mass	\bar{m}	1350 Kg
Vehicle Inertia	\bar{J}_z	1150 Kg \cdot m ²
Steering gear ratio	τ	1/10

TABLE II

MAGIC FORMULA'S COEFFICIENTS FOR TYPICAL ROAD CONDITIONS

Surface Type	B	C	D	E
Dry tarmac	10	1.9	1	0.97
Wet tarmac	12	2.3	0.82	1
Snow	5	2	0.3	1

IV. SIMULATION AND VALIDATION

The correctness and robustness of the proposed method are shown in this section, along with a comparison of its effectiveness for a benchmark using a standard disturbance rejection technique.

A. Vehicle Model Implementation

To show the effectiveness and robustness of the proposed method, the implementation of a real Robocar model is used by using the Vehicle Dynamics Blockset of the MATLAB/Simulink environment. The geometric and inertial parameters of the vehicle are listed in Table I. The interaction with the road surface is modeled by generating all lateral wheel forces, F_{yij} , via the nonlinear Pacejka tire model, the so-called the magic formula [26], i.e., $F_{yij} = F_{zij} \mu_{ij}$, with

$$\mu_{ij} = D \sin(C \arctan(B a_{ij} - E(B a_{ij} - \arctan(B a_{ij})))) \quad (19)$$

where B , C , D , and E are dimensionless coefficients whose values depend on the road surface (cf., Table II) for the typical values, also used here, to represent dry, wet, snow, and icy surfaces, and where are the vertical forces applied at each wheel. These last forces are given by

$$\begin{aligned} F_{z1j} &= (m/2l)(g a_2 - a_x h) + (-1)^j \Delta Z_1 \\ F_{z2j} &= (m/2l)(g a_1 + a_x h) + (-1)^j \Delta Z_2 \end{aligned}$$

for $j = 1, 2$, where g is the gravity acceleration, h is the height of the vehicle center of gravity with respect to the road and a_x is the vehicle's longitudinal acceleration in body frame, and Z_i are the lateral load transfers due to the suspensions, which are given by

$$\begin{aligned} \Delta Z_1 &= (d_1/t_1 l)(Y a_2 + N) + (k_{\phi_1}/k_{\phi})(h-d)Y \\ \Delta Z_2 &= (d_2/t_1 l)(Y a_1 - N) + (k_{\phi_2}/k_{\phi})(h-d)Y \end{aligned}$$

where l is the vehicle wheelbase, d_1 and d_2 are the front and rear no-roll center height, $k_{\phi} = k_{\phi_1} + k_{\phi_2}$, with k_{ϕ_1}

and k_{ϕ_2} being the front and rear suspension roll stiffness, respectively, and finally $d = (a_2 d_1 + a_1 d_2)/l$, $Y = Y_1 + Y_2$, $N = Y_1 a_1 - Y_2 a_2$. It should be noted that the roll and suspension effects on vehicle dynamics are taken into account via the lateral load transfers described above. Numerical values for the front and rear no-roll center height are $d_1 = 0.025$ m and $d_2 = 0.045$ m, respectively, with $k_{\phi_1} = 21740.6$ (N/rad) and $k_{\phi_2} = 22322.2$ N/rad.

Moreover, the wind force signal is obtained by modeling the wind speed u_w according to the stochastic Dryden model [4]. Specifically, the wind speed signal $u_w(t)$ is chosen to replicate turbulence at low altitudes, characterized by a height from the sea level of $h = 6$ m, an airspeed of $V = 50$ m/s, and a turbulence level of $W_{20} = 15$ kn. Moreover, to generate the wind moment signal, the lever arm x_w of the wind force is assumed to be a stochastic process with uniform distribution over the length of the vehicle, i.e., $-a_2 \leq x_w \leq a_1$. Accordingly, the wind force F_w and wind moment χ_w are obtained via the expressions

$$F_w = \frac{1}{2} \rho S C_y u_w^2, \quad \chi_w = F_w x_w$$

where $\rho = 1.225$ kg/m³ is the air density at sea level, $S = 2$ m² the so-called vehicle's lateral wetted area, $C_y = 1.5$ its lateral aerodynamic coefficient. Overall, the second equation of the lateral dynamics in 1 becomes $J \ddot{\psi} = a_1 Y_1(\delta_b) + a_2 Y_2(\delta_b) + \chi_w + N_x$, where $N_x = \Delta X_1 t_1 + \Delta X_2 t_2$, with $\Delta X_1 = (1/2)(F_{y11} \sin \delta_{11} - F_{y12} \sin \delta_{12})$ and $\Delta X_2 = (1/2)(F_{x22} - F_{x21})$, respectively.

B. Derivation of the DESO-Based Benchmark

The following benchmark based on the well-established theory described in [14] has been developed to compare the performance of our method with a *de-facto* standard disturbance rejection technique. It consists of a discrete-time implementation of the system obtained by the application of such a method, according to which an ADRC, based on an ESO, can be obtained as follows. First, consider an augmented state $\epsilon_k = (Z_k^T, w_k)^T$, including as an additional variable the disturbance w_k for which a dynamics must also be introduced. Assuming, as for our method, that only lateral position error measures, $y_{\epsilon_k} = e_k$, are available, and that, for a small delay of one sample, it holds $\delta_{k-1} \simeq \delta_k$ [24], a discrete-time ESO (DESO) is described by the iterative rule

$$\hat{\epsilon}_{k+1} = A_{\epsilon} \hat{\epsilon}_k + B_{\epsilon} \delta_{k-1} + L (y_{\epsilon_k} - C_{\epsilon} \hat{\epsilon}_k) \quad (20)$$

with

$$A_{\epsilon} = \begin{pmatrix} 1 & \lambda & 0 \\ 0 & 1 & \lambda \\ 0 & 0 & 1 \end{pmatrix}, \quad B_{\epsilon} = \lambda \begin{pmatrix} 0 \\ \bar{C}_1 \bar{\tau} / \bar{m} \\ 0 \end{pmatrix}, \quad C_{\epsilon} = (1 \quad 0 \quad 0)$$

where $L \in \mathbb{R}^3$ is such that the closed-loop dynamic matrix $A_{\bar{\epsilon}} = A_{\epsilon} - LC_{\epsilon}$ is Schur, ensures the asymptotic boundedness of the augmented state estimation error $\bar{\epsilon}_k = \hat{\epsilon}_k - \epsilon_k$, if, and only if, the following conditions are met: 1) (A_k, C_k) is fully observable; 2) w_k evolves as in $w_{k+1} = w_k + \lambda \kappa(\epsilon_k, w_k, k)$, where $\kappa(\epsilon_k, w_k, k)$ is a time-varying bounded function, i.e. $\exists M > 0$ s.t. $|\kappa(\epsilon_k, w_k, k)| \leq M \forall k$.

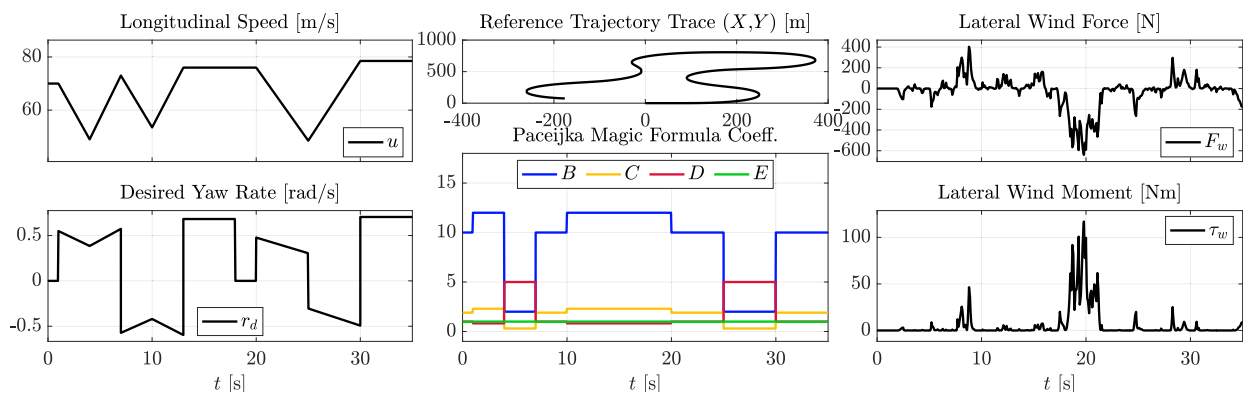


Fig. 3. Simulation scenario designed to test and assess the effectiveness and performance of the proposed methods. The longitudinal speed profile has alternating phases of acceleration and deceleration, and two plateau phases at quasi-constant velocities. The road surface ranges from dry, wet, and snow, while also highly varying wind gust force and moment have to be handled.

As a second step, once an estimate $\hat{\epsilon}_k = (\hat{Z}_k^T, \hat{w}_k)^T$ of the augmented state ϵ_k is retrieved via the DESO in (20), the steering control law

$$\delta_k = -\frac{\bar{m}}{\bar{C}_1 \bar{r}} (K \hat{Z}_k + \hat{w}_k) \quad (21)$$

with $K = (k_1, k_2)$ a free control gain, ensures the bounded stability of the full system

$$\begin{pmatrix} Z_{k+1} \\ \tilde{\epsilon}_{k+1} \end{pmatrix} = \begin{pmatrix} A_k & 0_{2 \times 3} \\ 0_{3 \times 3} & A_{\tilde{\epsilon}} \end{pmatrix} \begin{pmatrix} Z_k \\ \tilde{\epsilon}_k \end{pmatrix} + \begin{pmatrix} B_k \\ 0_{3 \times 1} \end{pmatrix} \delta_k + W_{\epsilon} \kappa(\epsilon_k, w_k, k) \quad (22)$$

with $W_{\epsilon} = \lambda (0_{1 \times 4}, 1)^T$, if, and only if, the signal $\kappa(\epsilon_k, w_k, k)$ is bounded. The convergence proof straightforwardly follows from standard arguments typical of the ADRC technique, but it is omitted here for the sake of space.

Finally, to obtain comparable behaviors for the proposed DUIO-based approach and the DESO-based one, the respective free control gains have been chosen so that the eigenvalues of the closed-loop matrix in (14) and that of (22) closed in the loop with (21) are in the similar locations. More specifically, without loss of generality, the speed of convergence of the lateral tracking errors has been tuned, via the control gain K , so that the eigenvalues of $A_k - B_v K$ are in $p_1 = (0.1, -0.1)$; simultaneously, the speed of convergence of the observers has been chosen to be ten times faster. In the DUIO case, this is obtained by placing the eigenvalues in $p_2 = (-0.01, 0.01)$ (and hence choosing $\sigma_1 = -0.01$ and $\sigma_2 = 0.01$) and, for the DESO, this is obtained by placing the eigenvalues in $p_3 = (-0.01, -0.01, 0.01)$ (and hence choosing l_1, l_2 , and l_3 accordingly).

C. Simulation and Testing With Vehicle Dynamics Blockset and Raspberry PI Board

The testing and validation scenario is reported in Fig. 3. The Robocar system is required to track a trajectory with a time-varying longitudinal speed $u(t)$ and curvature radius signal $\rho(t)$, under the presence of sudden wind gusts. The longitudinal speed profile reproduces a typical telemetry profile with acceleration and braking phases [9]; the time-varying

road friction is modeled via appropriate variation of the magic formula coefficients.

The goal of the testing is at least fourfold. First, it aims at showing the effectiveness of the proposed method as well as its robustness to unmodeled dynamics, parameter uncertainty, and measurement noise. For this purpose, the Robocar system is implemented as a double-track racecar by using the Vehicle Body 3-degree of freedom (DoF) block of vehicle dynamic blockset in MATLAB/Simulink [27]. Nominal values for the vehicle mass \bar{m} with a maximum variation of 45% from the real value are used in the numerical implementation of the estimators and controllers. Measurement noise is also added to the system outputs via the MATLAB/Simulink Random Source block, which generates pseudorandom Gaussian distributions [28]. Second, the testing aims at comparing the proposed approach with the above-described benchmark. Third, it aims at proving the real-time implementability of the solution and assessing the required computation time in terms of central processing unit (CPU) utilization, through a low-cost hardware setup, consisting of a Raspberry PI 4 Model B system. To achieve this, the proposed DUIO-based solution and the DESO-based benchmark are compiled for the Raspberry PI hardware, via the simulink real-time code generation, and built as standalone applications. The inclusion of both control methods represents a further computational load of the microcontroller, leading to an overestimate of the required CPU utilization and a further guarantee of the solution implementability. Finally, the testing intends to show if all the above-mentioned properties are maintained, even when enlarging the sampling time. For this reason, the scheduling times of the involved processes are chosen as $\lambda = 10^{-3}$ s and later as $\lambda = 10^{-2}$ s.

Figs. 4 and 5 report the results of the testing with $\bar{m}/m = 1.45$ and with scheduling times of $\lambda = 10^{-3}$ and $\lambda = 10^{-2}$, respectively. More precisely, Fig. 4 shows the DUIO always better estimates the state and the disturbance, at least by an order of magnitude. The resulting control is also much less affected by the noise and can better cope with the disturbance. Numerically, the integral time absolute error (ITAE) index computed on the tracking error and the disturbance estimation

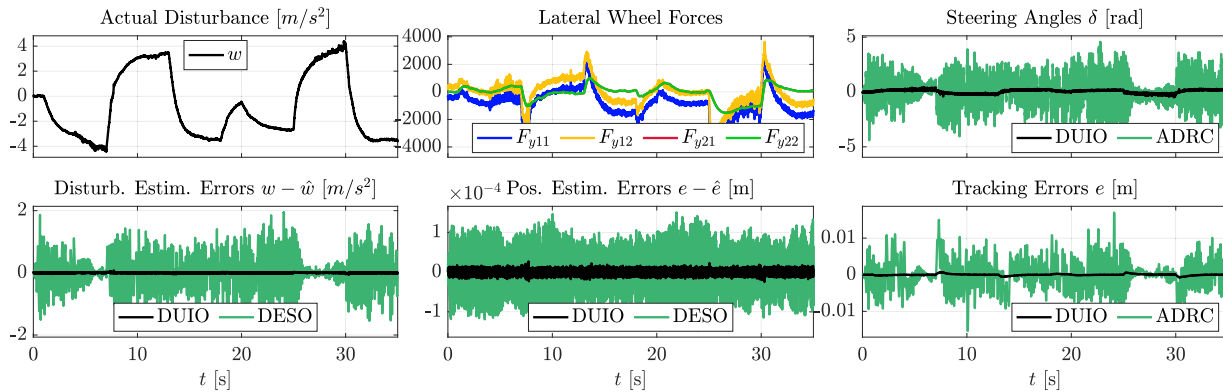


Fig. 4. Raspberry PI 4 testing with $\lambda = 10^{-3}$: results with noisy measures and a nominal mass $\bar{m}/m = 1.45$. The DUIO always obtains better estimates of the state and the disturbance, at least by an order of magnitude. The resulting control signal is also much less affected by the noise, better copes with the disturbance, and achieves improved tracking performance.

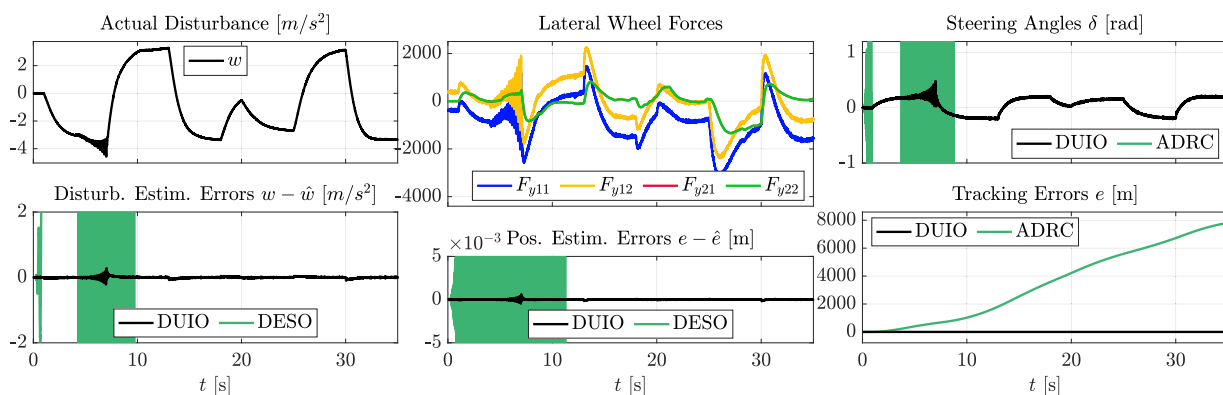


Fig. 5. Raspberry PI 4 testing with $\lambda = 10^{-2}$ the DESO-based benchmark is unable to correctly estimate and cope with the disturbance, which leads the system to instability (see the diverging green line of the tracking error). On the contrary, our proposed DUIO-based solution allows still a nice transient behavior and maintains stability.

TABLE III

ITAE INDEX COMPARISON FOR DUIO AND DESO-BASED APPROACHES, RESPECTIVELY, WITH SAMPLING TIME $\lambda = 10^{-3}$

Method	ITAE(e_{1k})	ITAE(\hat{w}_k)
DUIO	0.0791	5.523
DESO	2.031	294.8

error shows a clear superiority of the DUIO-based solution over the benchmark one (cf., Table III). The total CPU utilization, during the testing, for the two estimation and control processes is always less than 12.7% with a mean value of about 6.9%. Finally, Fig. 5 shows that when the scheduling time is increased to $\lambda = 10^{-2}$ s, the DESO-based benchmark is unable to correctly estimate and cope with the disturbance, which leads the system to instability (see the diverging green line of the tracking error). On the contrary, our proposed DUIO-based solution allows still a nice transient behavior and maintains stability.

V. CONCLUSION

A robust lateral controller for self-driving racecars was proposed using a delayed UIO. It showed robustness to

time-varying tire-road interface characteristics, wind gusts, and model uncertainty. Its closed-loop asymptotic stability was proven and its performance was compared to that of a disturbance estimation and rejection technique, for which only asymptotic boundedness was obtained. The solution requires no a-priori knowledge of the boundedness or the statistical properties of the system and measurement noises. Testing results confirmed the superior performance of the DUIO over a DESO, as expected from the literature [29]. Simulations further highlighted its superiority by showing that the DUIO-based control generates smoother control signals for the steering angle, leading to smaller and less spiky tracking errors than those of the ADRC methodology.

REFERENCES

- [1] M. Guiggiani, *The Science of Vehicle Dynamics*. Pisa, Italy: Springer, 2014, p. 15.
- [2] R. de Castro, R. E. Araújo, and D. Freitas, "Real-time estimation of tyre-road friction peak with optimal linear parameterisation," *IET Control Theory Appl.*, vol. 6, no. 14, pp. 2257–2268, Sep. 2012.
- [3] C. Bardawil, N. Daher, and E. Shamma, "Applying the similarity method on Pacejka's magic formula to estimate the maximum longitudinal tire-road friction coefficient," in *Proc. Amer. Control Conf. (ACC)*, Jul. 2020, pp. 218–223.
- [4] T. M. Ichwanul Hakim and O. Arifianto, "Implementation of Dryden continuous turbulence model into simulink for LSA-02 flight test simulation," *J. Phys., Conf. Ser.*, vol. 1005, Apr. 2018, Art. no. 012017.

- [5] M. Li, Y. Jia, and J. Du, "LPV control with decoupling performance of 4WS vehicles under velocity-varying motion," *IEEE Trans. Control Syst. Technol.*, vol. 22, no. 5, pp. 1708–1724, Sep. 2014.
- [6] G. Tagne, R. Talj, and A. Charara, "Design and comparison of robust nonlinear controllers for the lateral dynamics of intelligent vehicles," *IEEE Trans. Intell. Transp. Syst.*, vol. 17, no. 3, pp. 796–809, Mar. 2015.
- [7] C. M. Kang, W. Kim, and H. Baek, "Cascade backstepping control with augmented observer for lateral control of vehicle," *IEEE Access*, vol. 9, pp. 45367–45376, 2021.
- [8] F. Naets, S. van Aalst, B. Boulkroune, N. E. Ghouti, and W. Desmet, "Design and experimental validation of a stable two-stage estimator for automotive sideslip angle and tire parameters," *IEEE Trans. Veh. Technol.*, vol. 66, no. 11, pp. 9727–9742, Nov. 2017.
- [9] S. Pedone and A. Fagiolini, "Racecar longitudinal control in unknown and highly-varying driving conditions," *IEEE Trans. Veh. Technol.*, vol. 69, no. 11, pp. 12521–12535, Nov. 2020.
- [10] S. Li, J. Yang, W.-H. Chen, and X. Chen, *Disturbance Observer-Based Control: Methods and Applications*. Boca Raton, FL, USA: CRC Press, 2014.
- [11] S. Yu, J. Wang, Y. Wang, and H. Chen, "Disturbance observer based control for four wheel steering vehicles with model reference," *IEEE/CAA J. Autom. Sinica*, vol. 5, no. 6, pp. 1121–1127, Nov. 2018.
- [12] X. Wu, M. Zhang, and M. Xu, "Active tracking control for steer-by-wire system with disturbance observer," *IEEE Trans. Veh. Technol.*, vol. 68, no. 6, pp. 5483–5493, Jun. 2019.
- [13] R. Potluri and A. K. Singh, "Path-tracking control of an autonomous 4WS4WD electric vehicle using its natural feedback loops," *IEEE Trans. Control Syst. Technol.*, vol. 23, no. 5, pp. 2053–2062, Sep. 2015.
- [14] B.-Z. Guo and Z.-L. Zhao, *Active Disturbance Rejection Control for Nonlinear Systems: An Introduction*. Hoboken, NJ, USA: Wiley, 2016.
- [15] S. You, J. Gil, and W. Kim, "Fixed-time slip control with extended-state observer using only wheel speed for anti-lock braking systems of electric vehicles," *IEEE Trans. Intell. Transp. Syst.*, vol. 23, no. 7, pp. 6368–6378, Sep. 2022.
- [16] H. Wang, Z. Zuo, Y. Wang, H. Yang, and S. Chang, "Composite nonlinear extended state observer and its application to unmanned ground vehicles," *Control Eng. Pract.*, vol. 109, Apr. 2021, Art. no. 104731. [Online]. Available: <https://www.sciencedirect.com/science/article/pii/S0967066121000083>
- [17] S. E. Talole, J. P. Kolhe, and S. B. Phadke, "Extended-state-observer-based control of flexible-joint system with experimental validation," *IEEE Trans. Ind. Electron.*, vol. 57, no. 4, pp. 1411–1419, Apr. 2010.
- [18] Y. Wu, L. Wang, J. Zhang, and F. Li, "Path following control of autonomous ground vehicle based on nonsingular terminal sliding mode and active disturbance rejection control," *IEEE Trans. Veh. Technol.*, vol. 68, no. 7, pp. 6379–6390, Jul. 2019.
- [19] H. Yang, L. Cheng, Y. Xia, and Y. Yuan, "Active disturbance rejection attitude control for a dual closed-loop quadrotor under gust wind," *IEEE Trans. Control Syst. Technol.*, vol. 26, no. 4, pp. 1400–1405, Jul. 2018.
- [20] Y. Xia, F. Pu, S. Li, and Y. Gao, "Lateral path tracking control of autonomous land vehicle based on ADRC and differential flatness," *IEEE Trans. Ind. Electron.*, vol. 63, no. 5, pp. 3091–3099, May 2016.
- [21] W. Xue, W. Bai, S. Yang, K. Song, Y. Huang, and H. Xie, "ADRC with adaptive extended state observer and its application to air–fuel ratio control in gasoline engines," *IEEE Trans. Ind. Electron.*, vol. 62, no. 9, pp. 5847–5857, Sep. 2015.
- [22] S. Sundaram and C. N. Hadjicostis, "Delayed observers for linear systems with unknown inputs," *IEEE Trans. Autom. Control*, vol. 52, no. 2, pp. 334–339, Feb. 2007.
- [23] (2020). *Vehicle Dynamics Blockset*. [Online]. Available: <https://it.mathworks.com/products/vehicle-dynamics.html#full-vehicle>
- [24] K. Youcef-Toumi and O. Ito, "A time delay controller for systems with unknown dynamics," in *Proc. Amer. Control Conf.*, Jun. 1988, pp. 904–913.
- [25] D. Caporale et al., "A planning and control system for self-driving racing vehicles," in *Proc. IEEE 4th Int. Forum Res. Technol. Soc. Ind. (RTSI)*, Sep. 2018, pp. 1–6.
- [26] H. B. Pacejka, "Chapter 4—Semi-empirical tyre models," in *Tyre and Vehicle Dynamics*, H. B. Pacejka, Ed., 2nd ed. Oxford, U.K.: Butterworth-Heinemann, 2006, pp. 156–215. [Online]. Available: <https://www.sciencedirect.com/science/article/pii/B9780750669184500046>
- [27] (2021). *Vehicle Body 3DOF*. [Online]. Available: <https://it.mathworks.com/help/vdynblks/ref/vehiclebody3dof.html>
- [28] (2006). *Random Source*. [Online]. Available: <https://it.mathworks.com/help/dsp/ref/randomsource.html>
- [29] A. H. Al-Bayati and Z. Skaf, "A comparative study of linear observers applied to a DC servo motor," in *Proc. Int. Conf. Modelling, Identificat. Control*, Jul. 2010, pp. 785–790.